Materials Today Communications 30 (2022) 103216

Contents lists available at ScienceDirect

Materials Today Communications

journal homepage: www.elsevier.com/locate/mtcomm

# Fabrication of porous apatite-wollastonite glass ceramics using a two steps sintering process

Zafer Tatli [a], Oana Bretcanu [b], Fatih Çalışkan [a,*], Kenny Dalgarno [b]

[a] Metallurgical and Material Engineering, Faculty of Technology, Sakarya University of Applied Sciences, Sakarya, Turkey
[b] School of Engineering, Newcastle University, NE1 7RU Newcastle upon Tyne, UK

ARTICLE INFO

*Keywords:*
Bioceramics
Apatite - Wollastonite (AW)
Sintering
Porous materials

ABSTRACT

The aim of this work was to produce porous apatite-wollastonite (AW) glass-ceramic scaffolds via a two step sintering process and to assess their suitability for bone replacement applications. Apatite-wollastonite, polyvinyl chloride (PVC) and poly (methyl methacrylate) (PMMA) were used to fabricate bonelike porous scaffolds using the burning out method. Compression tests were carried out on AW scaffolds after sintering. Scanning electron microscopy was used to observe the pores distribution and microstructure of the sintered scaffolds. The scaffolds containing 70% AW and 30% PMMA have the highest compressive strength and apparent density. All scaffolds present a microstructure with interconnected micro and macroporosity (less than 50 μm).

## 1. Introduction

The first apatite-wollastonite (AW) glass-ceramic was obtained in 1980′s by controlled crystallization of MgO-SiO2-P2O5-CaO-CaF2 glass which was produced by conventional melt-quenching method. Since then this glass ceramic has been produced in various size and forms like powders and dense or porous blocks, obtained by powder sintering [1]. Bioactive glasses and glass–ceramics are widely studied due to their particular property of directly bonding to the human tissues, by forming a chemical bond with the implant. In fact some biomaterials, such as Bioglass®, AW and sintered hydroxyapatite, form a layer of hydroxyapatite on their surface, similar to the mineral phase of the natural bone, when they are implanted in natural tissues [2–7].

Bioactive inorganics phase can react with physiological fluids forming tenacious bonds to bone through the formation of bone-like HAp layers inducing effective biological interaction and fixation of bone tissue with the implant surface. Furthermore, in the event of silicate bioactive glasses such as 45S5 Bioglass®, the reactions at the graft surface are favourable intracellular and extracellular responses promoting rapid bone formation [8,9].

Bone has a natural ability to heal and remodel its microstructure in the absence of rigid fixation at the fracture site. This natural repair sometimes requires rigid fixation devices such as plates, nails, etc., to stabilize and realign large fractured bones. In many cases of major bone loss such as trauma, cancer, congenital abnormalities or bone deficiency, there is a requirement for bone replacements or fillers. To date, the most common bone reconstruction procedures still rely on bone grafts, including autograft and allograft, both cortical and cancellous [10]. The present golden standard in orthopaedic surgery are autografts obtained from the same patient, due to their rapid and completed osseous integration. However, they can be used only for small bone defects due to a limited material supply. Allografts obtained from human cadavers can be used for larger defects but they are often associated with morbidity and potential risk of immunogenic rejection and pathogens transfer from donor to host [11]. All these factors led to the development of synthetic grafting materials, which have the advantage of eliminating the problems with donor derived grafts.

A wide range of synthetic materials such as metals, alloys, polymers, glass and ceramics have been studied in recent years to replace or reinforce skeletal loss, although an ideal grafting material has not yet been developed. The ideal grafting material should display a series of characteristics including: biocompatibility; surface chemistry for cell attachment, proliferation, and differentiation; appropriate porosity and internal porous architecture to benefit vascularization; and comparable mechanical properties to natural bone tissues at the site of implantation [10].

Traditional ceramics such as alumina are usually biologically inert materials that form a thick layer of fibrous tissue after implantation which ultimately causes loosening of implants. Bioactive ceramics are promising for bone implantation because of their bioactivity and

* Corresponding author.
*E-mail address:* fcaliskan@subu.edu.tr (F. Çalışkan).

https://doi.org/10.1016/j.mtcomm.2022.103216
Received 7 June 2021; Received in revised form 10 January 2022; Accepted 28 January 2022
Available online 1 February 2022

**Table 1**
Density and particles size of ceramic and polymers powders.

| Powder | Density (g/cm$^3$) | Particle Size (μm) |
|---|---|---|
| AW | 3.08 | 45–90 |
| PVC | 1.4 | 5–100 |
| PMMA | 1.18 | 5–70 |

mechanical properties and have been widely used for bone substitution and regeneration [12].

Montazerian and Zanotto have investigated the main properties and the potential for use of bioactive glass-ceramics in orthopaedics and dentistry [13,14]. Bioactive glass-ceramic scaffolds have superior in vivo behaviour in terms of bone formation, mineralization, higher interfacial bonding between implant and bone according to the particular form glass or other bioactive scaffolds (HA, TCP) [8]. Previous work [15] has shown that porosities of 89.2 ± 1.4% together with mechanical strength of 0.18 ± 0.03 MPa can be achieved. The compressive strength of cancellous bone is in the range of 0.2–4.0 MPa when the relative density is ~ 0.1 [15]. While elastic modulus of cortical bone is 17 GPa, spongy bone is 350 MPa [16]. Wollastonite scaffolds have been produced using a replica method, with compressive strengths of 0.4 MPa and 3.6 MPa [14].

Sintering is a good manufacturing method to achieve porous products with appropriate mechanical strength. Although conventional sintering can produce porous bone implants, the restriction and difficulties in the production of free-form shape and a customisable implant that offers potential to provide improved bone defect repair modalities led to an alternative fabrication technology: rapid prototyping/manufacturing (RP/RM). Numerous other methods exist, including three dimensional (3D) printing, stereolithography and fused deposition modelling [5,17]. Another method commonly used to fabricate porous structures is indirect selective laser sintering [18,19]. A computer is essential to this process as initially a CAD model of the scaffold is produced. This information is then transferred to the laser sintering machine, which fabricates the scaffold layer by layer.

Sintering is an economic technique, suitable for automation and fabrication of complex parts with high densities. In this technique, the powder mixture is pressed into the desired shape and then sintered using appropriate heating treatments. Lower density porous structures can be produced by using the replication method [20,21]. In this process scaffolds are prepared by coating a 'sacrificial' polymer template with a ceramic slurry. After coating, any excess slurry is removed and the template is then dried and sintered. During sintering the polymer burns out whilst the ceramic sinters.

Scaffold fabrication process generally involves sintering steps, which requires the glasses to be heated above their glass transition temperature to initiate localized flow. Many bioactive glasses, including 45S5 Bioglass®, crystallize just above their Tg; therefore, sintered bioactive glass scaffolds are usually made of glass-ceramics [8,22].

Recently, a revised replication method has been developed [23,24]. The main difference in this process is the addition of polyethylene powder to the slurry. The excess slurry is not removed from the template after immersion. Generally this process seems to improve the mechanical properties of the scaffold.

The aim of this work was to produce porous glass-ceramic AW scaffolds via two-steps sintering and to assess their mechanical properties and microstructure. The two-steps sintering process consists in burning out the polymer, followed by sintering the glass-ceramic powder. A similar process is discussed in [20] and [25].

## 2. Experimental

In order to produce AW glass-ceramic scaffolds, commercially available AW powders (Glass Technology Services Ltd (GTS) Sheffield, UK), polyvinyl chloride (PVC, Sigma Aldrich) and poly (methyl methacrylate) (PMMA, Alpha Aesar GmbH &Co) powders were used. The density and particles size of each powder are given in Table 1.

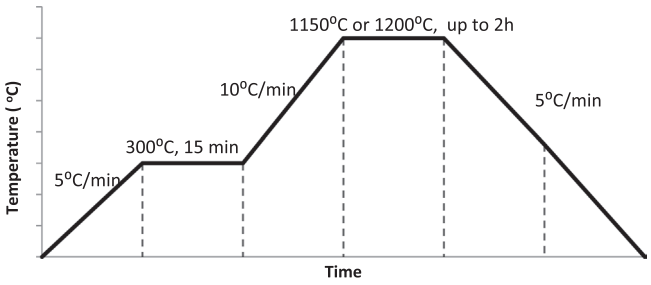


**Fig. 1.** Two steps sintering of AW-polymer mixtures.

**Table 2**
Density of scaffolds obtained after sintering of AW-polymer mixtures at 1150 °C for 2 h.

| Density (g/cm$^3$) | | | |
|---|---|---|---|
| AW-PVC | | AW-PMMA | |
| 70%AW-30%PVC | 2.07( ± 2.1%) | 70%AW-30%PMMA | 2.38( ± 2.0%) |
| 60%AW-40%PVC | 2.00( ± 2.4%) | 60%AW-40%PMMA | 2.30( ± 2.1%) |
| 50%AW-50%PVC | 1.92( ± 3.5%) | 50%AW-50%PMMA | 2.13( ± 2.4%) |

**Table 3**
Density of scaffolds obtained after sintering of AW-polymer mixtures at 1200 °C for 1 h.

| Density (g/cm$^3$) | | | |
|---|---|---|---|
| AW-PVC | | AW-PMMA | |
| 70%AW-30%PVC | 2.31( ± 2.1%) | 70%AW-30%PMMA | 2.49( ± 1.5%) |
| 60%AW-40%PVC | 2.28( ± 2.5%) | 60%AW-40%PMMA | 2.38( ± 2.0%) |
| 50%AW-50%PVC | 2.20( ± 2.7%) | 50%AW-50%PMMA | 2.25( ± 2.4%) |

To obtain porous structures 30%, 40% and 50% (volume %) polymer powders were mixed with AW powders and then pressed in a cold press, obtaining pellets with a 16 mm diameter and 6 mm height. These pellets were then pressed in a cold isostatic press (250 MPa) (CIP Stansted Fluid Company, UK) to get denser green compacts. The resultant green compacts were then sintered at temperatures up to 1200 °C for a maximum of 2 h, using a two step sintering process. After sintering, the compressive strength of the resulted AW scaffolds was tested using a Zwick/Roell universal testing machine, with a 250 kN load cell. Compression test results are the arithmetic mean value of 5 samples prepared under the same conditions.

The microstructure of the sintered scaffolds was observed using a scanning electron microscope (Hitachi 2400). The apparent density of ceramic scaffolds was measured using the method described by the ASTM C373 standard. Density of each sample was measured 5 times and mean value of density was arithmetically calculated.

## 3. Results and Discussions

AW scaffolds were sintered at temperatures up to 1200 °C. At temperatures above 1200 °C the pellets started to collapse and lost their original shape due to melting of the ceramic particles. A representative two step sintering process is presented in Fig. 1. A heating rate of 5 °C/min was used for the first step (up to 300 °C), which was designed to burn out the polymers. The second step was carried out using a heating rate of 10 °C/min up to either 1150 °C or 1200 °C, for AW powder sintering.

The densities of the AW scaffolds after sintering at 1150 °C and 1200 °C are presented in Tables 2 and 3. The apparent density results show that pellets containing PMMA have higher density than the ones

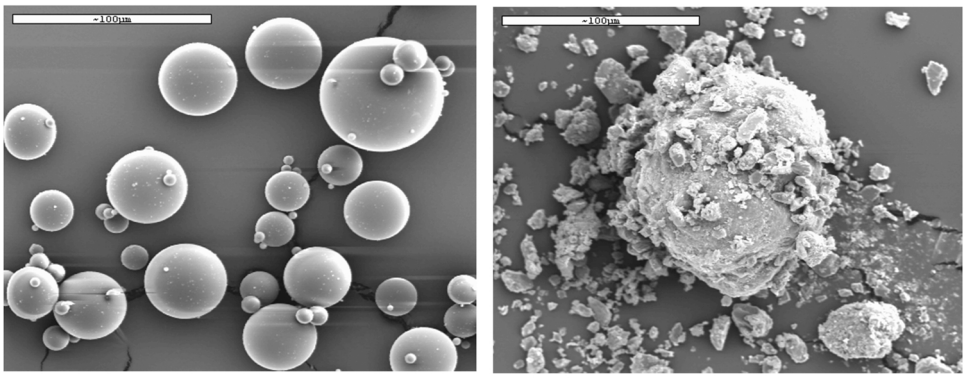


**Fig. 2.** SEM images of a) PMMA and b) PVC powders at 200X magnification.

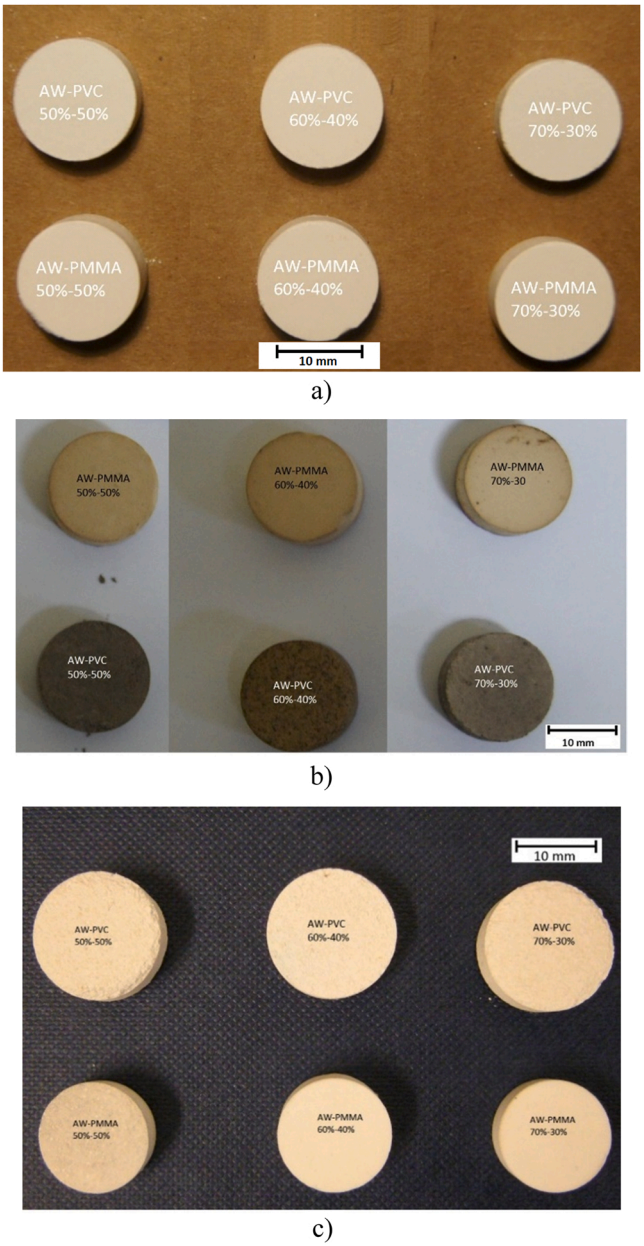


**Fig. 3.** AW-polymer pellets a) before sintering, b) after first step sintering process (polymer burning) at 300 °C for 15 min and c) after second step sintering at 1200 °C for 1 h.

containing PVC after sintering at both 1150 °C and 1200 °C temperatures. As expected, as the polymer content increases, the apparent density decreases, as the polymer burns out to leave a more porous structure. The apparent density of the sintered pellets is highest at the higher sintering temperature. The highest density (2.49 g/cm$^3$) is obtained for 70%AW-30%PMMA samples sintered at 1200 °C for 1 h.

SEM images of the two polymer powders PVC and PMMA, used for fabrication of AW-polymer pellets, are illustrated in Fig. 2. PMMA powders have regular spherical shape while PVC powders are irregular, having sharp edges. The particles size of PMMA powders varies in the range 5–70 µm (Fig. 2**a**), while PVC particles size is between 5 and 100 µm (Fig. 2**b**).

Images of AW-polymer pellets before heat treatment are shown in Fig. 3**a**. After the first heat treatment step (Fig. 3**b**) all pellets have a darker colour due to incomplete burning of the polymeric phase. It seems that AW-PVC samples have a darker colour presumably due to a higher amount of carbon entrapped in the pores. No shrinkage was observed for these samples after the first step heat treatment step at 300 °C. After sintering at 1200 °C for 1 h (Fig. 3**c**) all samples have a lighter colour, with the burn out of the polymeric phase completed. The AW-PMMA pellets shrunk approximately 20%, more than AW-PVC samples.

SEM images of the sintered pellets are shown in Fig. 4. AW-PMMA pellets have higher porosity and more regular spherical macropores than AW-PVC samples. AW-PVC samples seem to have smaller macropores than AW-PMMA samples after sintering under the same conditions (Fig. 4**b, d and f**). Both 60% AW- 40% PMMA and 70% AW- 30% PMMA samples have a homogeneous structure with well distributed macro and micropores (Fig. 4**c and e**).

It is seen that pores in the structure of the AW-PMMA are homogeneously distributed in the all along the sample (Fig. 4). The average pore sizes were measured as 32,4 µm, 26,8 µm and 28 µm, respectively, for the AW-PMMA samples whereas 39,4 µm 37,25 µm and 31,8 µm at 1150 ℃, 1175 ℃ and 1200 ℃ in the examination performed with an optical microscope.

In all samples, the pores have gradually become smaller with the increase in the holding temperature and the smallest size was reached 28 µm in the mean size for the AW-PMMA scaffold. In addition, while the highest difference in the average pore size between the AW-PMMA/-PVC was 10,45 µm at 1175 ℃. This means a 39% coarser pore size in the AW-PVC than in the AW-PMMA. It is also accepted that the highly porous structure (the open/close pore ratio, the amount of interconnected pores) eases passing of body fluids and nutrients into cells [9].

While the number of pores along the 1-inch line in the AW-PMMA was 279, there was 172 in the AW-PVC at 1150 ℃. At 1200 ℃, this value for the AW-PMMA (229) was also higher than for the AW-PVC (170). That is to say, the increase in the plateau temperature during

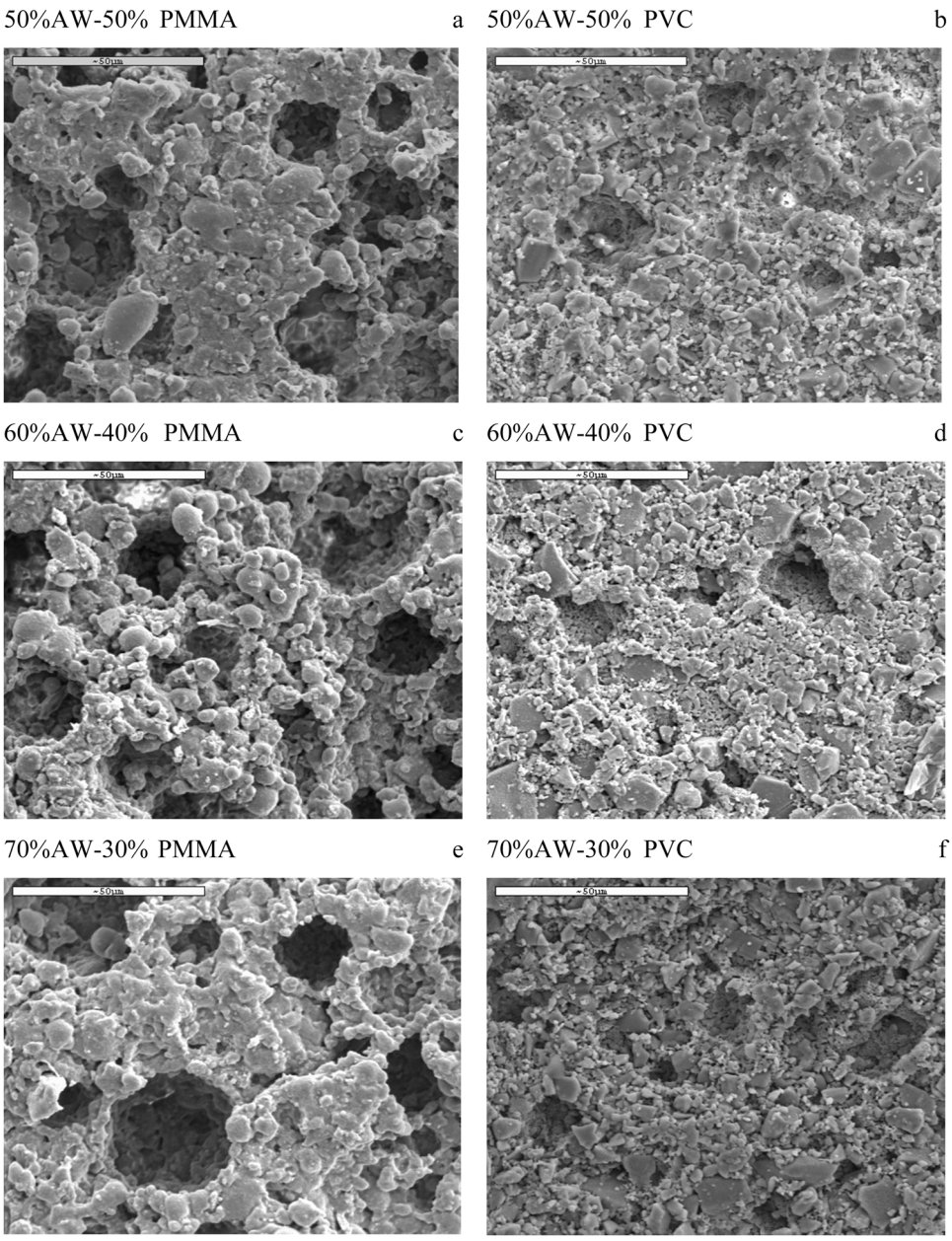


**Fig. 4.** SEM picture of fracture surface a) 50%AW-50%PPMMA, b) 50%AW-50%PVC, c) 60%AW-40% PMMA, d) 60%AW-40%PVC, e) 70%AW-30%PMMA f) 70% AW-30%PVC, sintered at 1200 °C for 1 h. (1000X magnification).

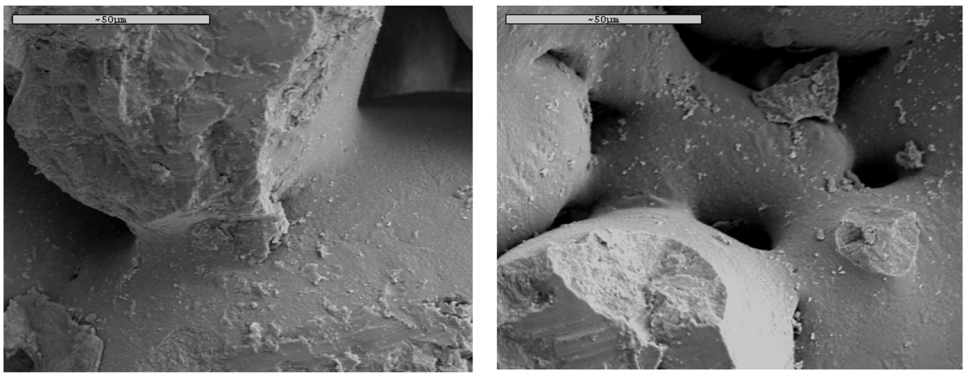


**Fig. 5.** SEM photos of AW powders sintered at 1200 °C for 30 min without polymers addition (1000X).

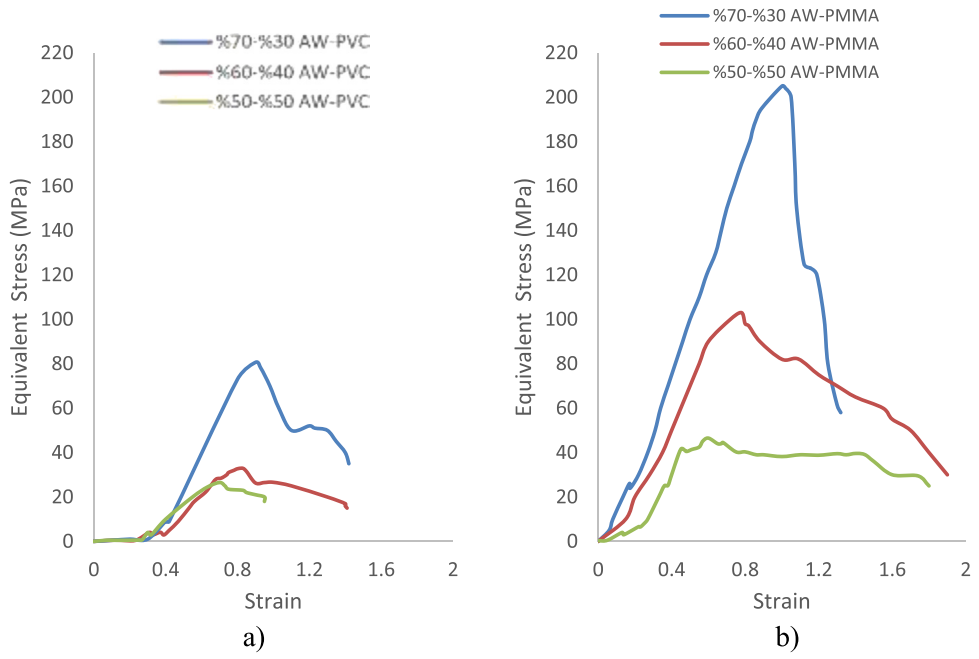


**Fig. 6.** Compression test of a) AW-PVC scaffolds and b) AW-PMMA scaffolds, sintered at 1200 °C for 1 h.

**Table 4**
Compressive strength of the samples, density and elastic modulus of the AW-PMMA/PVC scaffolds compared to that of bone.

| | Density (g/cm$^3$) | Total Porosity (%) | Compressive Strength (MPa) | Elastic Modulus (GPa) |
|---|---|---|---|---|
| [a]AW-PMMA | 2.49 | 21 | 205 (195–215 ± 5%) | 2.83 (2,68–2,97) |
| [b]AW-PVC | 2.31 | 32 | 80.6 (76–89 ± 10.1%) | 0.79 (0,71–0,87) |
| Cortical Bone | 1.6–2 | 5–30 | 130–200 | 12–20 |
| Trabecular Bone | 0.03–0.12 | 70–95 | 0.1–16 | 0.04–1 |

[a] 70% AW-30% PMMA.
[b] 70% AW-30% PVC after sintering at 1200 °C.

sintering caused a reduction in both the number of pores and the pore size.

A clear example of necking (sintered bridges) after sintering is shown in Fig. 5 for AW powders sintered at 1200 °C for 30 min without polymer additions. Interconnected pores (less than 50 μm) are visible in both pictures (Fig. 5**a and b)**. Without the polymer addition the sintering time of AW powders is 30 min. Longer sintering time produced a collapse of the structure due to powders melting.

Compression test graphs for AW-polymer pellets after sintering are presented in Fig. 6. The AW-PMMA samples have higher compressive strength than AW-PVC samples, probably due to a higher densification achieved after sintering. Compressive strength increases with the AW content. The highest value of compressive strength (205 MPa) was obtained for 70%AW-30% PMMA samples (Fig. 6**b**), which has the lower amount of PMMA. Considering the AW-PVC mixtures, the highest value of compressive strength (80 MPa) was obtained for 70%AW-30% PVC sample (Fig. 6**a**). Increasing the polymer content, the compressive strength decreases while the porosity increases. In the case of glass-ceramics obtained by a sintering process, during the occurrence of crystallization and densification, the microstructure of the parent glass shrinks, porosity is reduced and the solid structure gains mechanical strength [26].

AW/PMMA ratio can be varied to obtain strength and porosity values similar to the ones of the natural bone. The micro and macroporosity of ceramic scaffolds have vital roles in bone regeneration [27]. In order to optimise the polymeric phase, the maximum porosity needs to be achieved whilst the scaffold still meets the required mechanical properties. Generally, a denser structure should improve the mechanical stability of the scaffolds [28].

The porosity ratio of the 70% AW-30% PMMA sample after sintering at 1200 ℃ was calculated as approximately 21% while the porosity ratio of the 70% AW-30% PVC sample was calculated as approximately 31% **(**Table 4**).** The porosity amount of the porous is more compatible with spongy bone (trabecular bone) (70–95%). It is similar to trabecular architecture of cancellous bone. The density of the samples also matches that of cortical bone (1.6–2 g/cm$^3$) [16,29].

There are interconnected macropores (porosity 23.5–50%) in the scaffolds, with compressive strength values between 20 and 150 MPa. Compressive strength value (205 MPa for the AW-PMMA) found in this study is similar for bioactive glass-ceramic scaffolds. Moreover, the scaffolds formed from $SiO_2$-$P_2O_5$-CaO-MgO-$Na_2O$-$K_2O$ bioactive glass had a compressive strength of 1.3–5.4 MPa (with replication technique) [30–33].

It can be concluded from these results that the AW glass-ceramic scaffold (70% AW-30% PMMA) developed in the present study has a higher compressive strength and elastic modulus than both cortical bone and trabecular bone.

In all samples, an increase in the amount of pore-forming agent causes a decrease in density. Therefore, the decrease in the effective area carrying the load in the porous structure contributes to the decrease in the mechanical properties.

There is a meaningful difference between AW-PMMA and AW-PVC samples in terms of mechanical properties. The difference in mechanical performance of the bone-like structure of Apatite wollastonite glass-ceramic is thought to be due to the uniform distribution of the pores, the almost spherical pore morphology, and the narrow size distribution. In addition, compared to AW-PVC, this superior behavior of AW-PMMA scaffold can also be attributed to minimal pore contact with each other as clearly seen in Fig. 4**.**

In general, high number and size of pores means deteriorating in mechanical properties. But the quantification of the pore in a body is not enough to evaluate the resulting properties. The qualification of the

pores is at least as effective as its quantification. Looking at Fig. 4, a significant difference was seen in the pore structure as well as the pore amount between the AW-PMMA and AW-PVC samples. It may not be sufficient to attribute the significant difference in mechanical properties only to the amount of pores. Therefore, the difference in mechanical performance can be attributed to the spherical pore morphology and the uniform and the smaller average pore size in the sample. Irregular pore morphology in the AW-PVC can be due to the PVC powder size distribution and shapes (Fig. 2**b).**

## 4. Conclusions

AW-polymer mixtures can be successfully sintered using a two-step sintering process. At the end of the sintering process porous scaffolds are produced. The PMMA polymer powders used as a pore forming additive in the sintering process provide better mechanical properties in compression for the same volume of polymer added, and better defined porous structures, than PVC powders. 70% AW-30% PMMA mixtures have good mechanical properties and microporosity, which could be useful for bone scaffolds.

## CRediT authorship contribution statement

**Fatih Çalışkan:** Methodology, Writing – review & editing, Exprimental Studies. **Zafer Tatlı:** Methodology, Supervisor. **Oana Bretcanu:** Writing – review & editing, Exprimental studies. **Kenny Dalgarno:** Methodology, Supervisor.

## Declaration of Competing Interest

The authors declare that they have no known competing financial interests or personal relationships that could have appeared to influence the work reported in this paper.

## References


[1] T. Kokubo, S. Ito, M. Shigematsu, S. Sakka, T. Yamamuro, Mechanical-properties of a new type of apatite-containing glass-ceramic for prosthetic application, J. Mater. Sci. 20 (1985) 2001–2004, https://doi.org/10.1007/BF01112282.

[2] W. Cao, L.L. Hench, Bioactive materials, Ceram. Int. 22 (1996) 493–507, https://doi.org/10.1016/0272-8842(95)00126-3.

[3] L.L. Hench, Bioceramics, J. Am. Ceram. Soc. 81 (1998) 1705–1728, https://doi.org/10.1111/j.1151-2916.1998.tb02540.x.

[4] L.L. Hench, Bioceramics, a clinical success, Am. Ceram. Soc. Bull. 1 (7) (1998) 67–74 (VII).

[5] L.L. Hench, Bioceramics: from concept to clinic, J. Am. Ceram. Soc. 74 (1991) 1487–1510, https://doi.org/10.1111/j.1151-2916.1991.tb07132.x.

[6] B.D. Ratner, A.S. Hoffman, F.J. Schoen, J.E. Lemons, Biomaterials science, An Introduction to Materials in Medicine, Elsevier Academic Press,, 2004.

[7] P.N. De Aza, A.H. De Aza, P. Pena, S. De Aza, Bioactive glass and glass–ceramics, Ceramica y Vidro, Bolletin Soc. Esp. Ceram. 46 (2) (2007) 45–55, https://doi.org/10.4028/www.scientific.net/MSF.293.37.

[8] L.C. Gerhardt, A.R. Boccaccini, Bioactive glass and glass-ceramic scaffolds for bone tissue engineering, Materials 3 (2010) 3867–3910, https://doi.org/10.3390/ma3073867.

[9] E. Yilmaz, F. Caliskan, A new functional graded dental implant design with biocompatible and antibacterial properties, Mater. Chem. Phys. 277 (2022), 125481, https://doi.org/10.1016/j.matchemphys.2021.125481.

[10] S. Yang, K.F. Leong, Z. Du, C.K. Chua, The Design of Scaffolds for Use in Tissue Engineering, Part I. Traditional Factors, Tissue Eng. 7 (6) (2004) 679–689.

[11] M. Victor, M.D. Goldberg, M.D. Sam Akhavan, in: Jay R. Lieberman, Gary E. Friedlaender (Eds.), Biology of bone grafts in bone regeneration and repair, Humana Press, Totowa, N.J., 2005, pp. 57–65.

[12] A.J. Salgado, O.P. Coutinho, R.L. Reis, Bone Tissue Engineering State of the Art and Future Trends (https://doi:), Macromol. Biosci. 4 (2004) 743–765, https://doi.org/10.1002/mabi.200400026.

[13] M. Montazerian, E.D. Zanotto, History and trends of bioactive glass-ceramics (https://doi:), J. Biomed. Mater. Res. A 104 (2016) 1231–1249, https://doi.org/10.1002/jbm.a.35639.

[14] G. Kaura, V. Kumar, F. Baino, J. Mauro, G. PickrelleIain, E.O. Bretcanuf, Mechanical properties of bioactive glasses, ceramics, glass-ceramics and composites: State-of-the-art review and future challenges (https://doi:), Mater. Sci. Eng. C. 104 (2019), 109895, https://doi.org/10.1016/j.msec.2019.109895.

[15] L. Siqueira, L. Grenho, M.H. Fernandes, F.J. Monteiro, E.S. Trichês, 45S5 Bioglass-derived glass-ceramic scaffolds containing niobium obtained by gelcasting method, Mat. Res. 24 (2021) 1, https://doi.org/10.1590/1980-5373-MR-2020-0403.

[16] Y.S. Lai, W.C. Chen, C.H. Huang, C.K. Cheng, K.K. Chan, T.K. Chang, The effect of graft strength on knee laxity and graft in-situ forces after posterior cruciate ligament reconstruction, Public Libr. Sci. 10 (5) (2015), e0127293, https://doi.org/10.1371/journal.pone.0127293.

[17] E. Sachlos, J.T. Czernuszka, S. Gogolewski, M. Dalby, Making tissue engineering scaffolds work, Review: on the application of solid freeform fabrication technology to the production of tissue engineering scaffolds, Eur. Cells Mater. Vol. 5 (2003) 29–40.

[18] K.H. Tan, C.K.C.K.F. Leong, M.W. Naing, and C.M. Cheah, Fabrication and characterization of three-dimensional poly(ether–ether–ketone)/–hydroxyapatite biocomposite scaffolds using laser sintering. Proc. IMechE,. 219 (Engineering in Medicine): p. 183–194, 2005.

[19] K. Xiao, K.W. Dalgarno, D.J. Wood, R.D. Goodridge, C. Ohtsuki, Indirect selective laser sintering of apatite–wollostonite glass–ceramic, Proc. Inst. Mech. Eng., Part H: J. Eng. Med. (2008) 9.

[20] D. Mohamad Yunos, O. Bretcanu, A.R. Boccaccini, Polymer-bioceramic composites for tissue engineering scaffolds, J. Mater. Sci. 43 (2008) 4433, https://doi.org/10.1007/s10853-008-2552-y.

[21] Q.Z. Chen, I.D. Thompson, A.R. Boccaccini, 45S5 Bioglass®-derived glass–ceramic scaffolds for bone tissue engineering, Biomaterials 27 (11) (2006) 2414–2425, https://doi.org/10.1016/j.biomaterials.2005.11.025.

[22] C. Vitale-Brovarone, E. Verné, L. Robiglio, P. Appendino, F. Bassi, G. Martinasso, et al., Development of glass-ceramic scaffolds for bone tissue engineering: characterisation, proliferation of human osteoblasts and nodule formation, Acta Biomater. 3 (2007) 199–208, https://doi.org/10.1016/j.actbio.2006.07.012.

[23] D. Bellucci, A.S, V. Cannillo, A Revised Replication Method for Bioceramic Scaffolds (https://doi:), Bioceram. Dev. Appl. 1 (2011) 8, https://doi.org/10.4303/bda/D110401.

[24] D. Bellucci, V. Cannillo, A. Sola, Shell Scaffolds: A new approach towards high strength bioceramic scaffolds for bone regeneration (https://doi:), Mater. Lett. 64 (2) (2010) 203–206, https://doi.org/10.1016/j.matlet.2009.10.054.

[25] J.A. Dyson, P.G. Genever, K.W. Dalgarno, D.J. Wood, Development of custom-built bone scaffolds using mesenchymal stem cells and apatite-wollastonite glass-ceramics, Tissue Eng. 13 (2007) 12, https://doi.org/10.1089/ten.2007.0124.

[26] I.D. Thompson, L.L. Hench, Mechanical properties of bioactive glasses, glass-ceramics and composites (https://doi:), Proc. Inst. Mech. Eng. Part H. -J. Eng. Med. 212 (1998) 127–136, https://doi.org/10.1243/0954411981533908.

[27] J.R. Woodard, et al., The mechanical properties and osteoconductivity of hydroxyapatite bone scaffolds with multi-scale porosity, Biomaterials 28 (1) (2007) 45–54. ⟨https://doi:0.1016/j.biomaterials.2006.08.021⟩.

[28] S. Bose, et al., Pore size and pore volume effects on alumina and TCP ceramic scaffolds (https://doi:), Mater. Sci. Eng.: C. 23 (4) (2003) 479–486, https://doi.org/10.1016/S0928-4931(02)00129-7.

[29] Q. Grimal, P. Laugier, Quantitative ultrasound assessment of cortical bone properties beyond bone mineral density, Irbm 40 (2019) 16–24, https://doi.org/10.1016/j.irbm.2018.10.006.

[30] C. Vitale-Brovarone, F. Baino, E. Verné, High strength bioactive glass-ceramic scaffolds for bone regeneration, J. Mater. Sci. Mater. Med. 20 (2009) 643–653, https://doi.org/10.1007/s10856-008-3605-0.

[31] Q. Fu, M.N. Rahaman, B.S. Bal, R.F. Brown, Preparation and in vitro evaluation of bioactive glass (13-93) scaffolds with oriented microstructures for repair and regeneration of load-bearing bones, J. Biomed. Mater. Res. Part A. 93A (2010) 1380–1390, https://doi.org/10.1002/jbm.a.32637.

[32] F. Baino, E. Verné, C. Vitale-Brovaron, 3-D high-strength glass-ceramic scaffolds containing fluoroapatite for load-bearing bone portions replacement (https://doi:), Mater. Sci. Eng. C. 29 (2009) 2055–2062, https://doi.org/10.1016/j.msec.2009.04.002.

[33] F. Baino, G. Novajra, C.V. Brovarone, Bioceramics and scaffolds: a winning combination for tissue engineering (https://doi:), Front Bioeng. Biotechnol. 3 (2015) 202, https://doi.org/10.3389/fbioe.2015.00202.